Threats to coastal communities of Mahanadi delta due to imminent consequences of erosion – present and near future.

Anirban Mukhopadhyay*, Pramit Ghosh, Abhra Chanda, Amit Ghosh, Subhajit Ghosh, Shouvik Das, Tuhin Ghosh ,Sugata Hazra

School of Oceanographic Studies, Jadavpur University, Kolkata, West Bengal, India

*Corresponding author: **anirban_iirs@yahoo.com**

Abstract: Coastal erosion is a natural hazard which causes significant loss to properties as well as coastal habitats. Coastal districts of Mahanadi delta, one of the most populated deltas of the Indian subcontinent, are suffering from the ill effects of coastal erosion. An important amount of assets is being lost every year along with forced migration of huge portions of coastal communities due to erosion. An attempt has been made in this study to predict the future coastline of the Mahanadi Delta based on historical trends. Historical coastlines of the delta have been extracted using semi-automated Tasselled Cap technique from the LANDSAT satellite imageries of the year 1990, 1995, 2000, 2006 and 2010. Using Digital Shoreline Assessment System (DSAS) tool of USGS, the trend of the coastline has been assessed in the form of End Point Rate (EPR) and Linear Regression Rate (LRR). A hybrid methodology has been adopted using statistical (EPR) and trigonometric functions to predict the future positions of the coastlines of the years 2020, 2035 and 2050. The result showed that most of the coastline (≈65%) is facing erosion at present. The predicted outcome shows that by the end of year 2050 the erosion scenario will worsen which in turn would lead to very high erosion risk for 30 % of the total coastal mouzas (small administrative blocks). This study revealed the coastal erosion trend of Mahanadi delta and based on the predicted coastlines it can be inferred that the coastal communities in near future would be facing substantial threat due to erosion particularly in areas surrounding Puri (a renowned tourist pilgrimage) and Paradwip (one of the busiest ports and harbours of the country).

Key words: coastal erosion, coastal communities, DSAS, EPR, LRR, Mahanadi Delta

1. Introduction

Shorelines are defined as the interface between sea and land. Due to various natural (like storm surges, sea level rise, flood etc.) and anthropogenic factors (like construction of jetties and ports, clearing of coastal vegetation ec.), shorelines are undergoing unprecedented change throughout the world. Around 70% of the world's shorelines are undergoing coastal erosion, resulting in instability in these regions and affecting the socio-economic setup of the regions concerned (IPCC 2001). Whenever any natural processes taking place in these shorelines threatens human life and infrastructure it leads to natural hazards and in order to prevent the impact of such hazards coastal managers should know the intrinsic physical, ecological and coastal features, human occupation, population, demographic details along with past and present shoreline trends (Jana and Bhattacharya, 2012). This demands an assessment of the coastal dynamics especially at regional levels so that stability can be reinstated and natural disasters like floods could be avoided in the future.

Most research on coastal management principally relies upon historical shoreline data (Addo et al., 2008). Natural causes of shoreline change include storms, floods, morphology and geology of the catchment areas, their size and the nature of the sedimentation basin – all of which affects coastal erosion (Kumar et al., 2010). According to Albert and Jorge (1998), climate change induced rainfall along with the coastal hydrodynamics such as waves, tides and currents also result in shoreline change. Changes in hydrodynamics of near-shore environment like river mouth processes, storm surges and the nature of coastal landforms also regulate the degree of shoreline change (Scott, 2005; Narayana and Priju, 2006; Kumar and Jayappa, 2009). Man-made factors include construction of jetties, groins, ports, industries, sea-walls and aquaculture farming which usually lead to widespread erosion by altering the sediment movement along the coast

(Kumar et al., 2010). Sea-level rise is also a major cause of coastal erosion. Although it may not be perceptible to the human eye mainly because of its slow rate, its effect is prominent when shorelines are compared after a long time interval (Hazra et al., 2002; Feagin et al., 2005).

Vulnerable coastal ecosystems such as mangroves are rapidly undergoing loss all over the globe (Lovelock et al., 2015). Shoreline erosion due to sea-level rise is directly affecting these ecosystems (Huq et al. 1995). Sea-level has increased globally at the rate of approximately 1.8 mm/year between the years 1950 and 2000 (Church et al., 2004) although this rate was found to vary in different parts of the world (Church et al., 2008). By the end of the 21st century, sea-level is projected to increase by 0.18 – 0.59m compared to 1980-1999 levels according to IPCC (Solomon et al., 2007). Rahmstorf et al. (2007) expects sea-level rise, mainly due to global warming, will continue for centuries. In fact, some researchers are assuming that this change would be more than that predicted by IPCC (Pfeffer et al., 2008; Rahmstorf, 2007; Kay et al., 2015; Lovelock et al., 2015).

Hence it is of paramount importance to assess these changes in the coastlines so that their effects on the ecology as well as human society can be attenuated. Taking proper measures to stop the rapid erosion occurring due to various factors by immediate implementation of policies also require identifying the most vulnerable areas and the magnitude of the rate of erosion. It is also important to measure the coastal erosion/accretion for a wide-range of studies, like development of setback planning, hazard zoning, erosion-accretion studies, and predictive modelling of coastal morphodynamics (Sherman & Bauer, 1993; Al Bakri, 1996; Zuzek et al., 2003).

Remote sensing data has been used widely in many previous studies in order to analyse the temporal variability of shoreline positions (Dolan et al., 1991; Fletcher et al.,

2003; Thieler and Danforth, 1994; Ford, 2013). A popular shoreline assessment tool namely Digital Shoreline Analysis System (DSAS) developed by Woods Hole Coastal and Marine Science Center, USGS was implemented in this study to assess the coastline change in one of the most vulnerable shorelines in India, namely Mahanadi delta. Keeping in view the above mentioned background, it was hypothesized that the shoreline of Mahanadi Delta facing the Bay of Bengal underwent substantial erosion at par with the global erosion rate (Ericson et al., 2006; Syvitski et al., 2009). The main aim of the study was to understand the existing and future risk of coastal erosion in the Mahanadi Delta. Based on the proposed hypothesis the following objectives were formulated for the present study. The first objective of the study was i) to measure the erosion rates of this shoreline (between the years 1990 and 2015 using satellite images) (Table 1) by means of two statistical techniques namely End-Point Rate (EPR) and Linear Regression Rate (LRR) and identify which method is suitable for the present study area, ii) to predict the future position of shorelines for the years 2035 and 2050 and iii) to prepare a risk map for the years 2035 and 2050 keeping in view the demographic factors in addition to shoreline change scenarios, in order to identify the areas which will be hard hit due to erosion activities.

2. Materials and methods

2.1 Study Area

Flowing for over 900 km, the Mahanadi River basin is over 1,40,000 km^2 in area and extends over seven states of India (Fig. 1). It is known to deposit the most silt than any other rivers in the Indian subcontinent (Mahalik and Maejima 1996; Mahalik 2000). The delta's fluvial upper portion is primarily composed of sediments deposited from the rivers in the region. The fluvial features can be segmented into major active river systems

– Birupa, Mahanadi and Kathjodi-Debi systems. The drainage channels and the flood plains are the other major geographical features of the fluvial portion of the delta. Apart from the fluvial portion, there are ancient beach ridges, tidal flats along the coast with mangroves. These fluvio-marine features are found running parallel to the coastline (Somanna, 2013). The Mahanadi delta is a meso tidal delta and the tidal range varies from 2 to 3 metre. (Mahalik et al. 1996, Kumar and Bhattacharya 2004)

Mahanadi Delta, while being vulnerable on one hand, is also one of the most populated river deltas of India. The area has one of the most fertile agricultural lands and contributes positively to the national economy. Rice, oilseeds and sugarcane are the main crops produced in this delta. Good transportation network of the state helps in trading of these crops through the nearby well-developed cities of Cuttack and Sambalpur. This trading facilitates the welfare of the local agricultural community who earn their livelihood mainly through the sale of their crops in these cities. Floods have been a perennial problem in this delta. Puri, a city in the Mahanadi delta, being an active pilgrimage site, attracts a voluminous footfall in the region. Coastal erosion is, therefore, a threat to historically and culturally important buildings such as the centuries-old Puri temple.

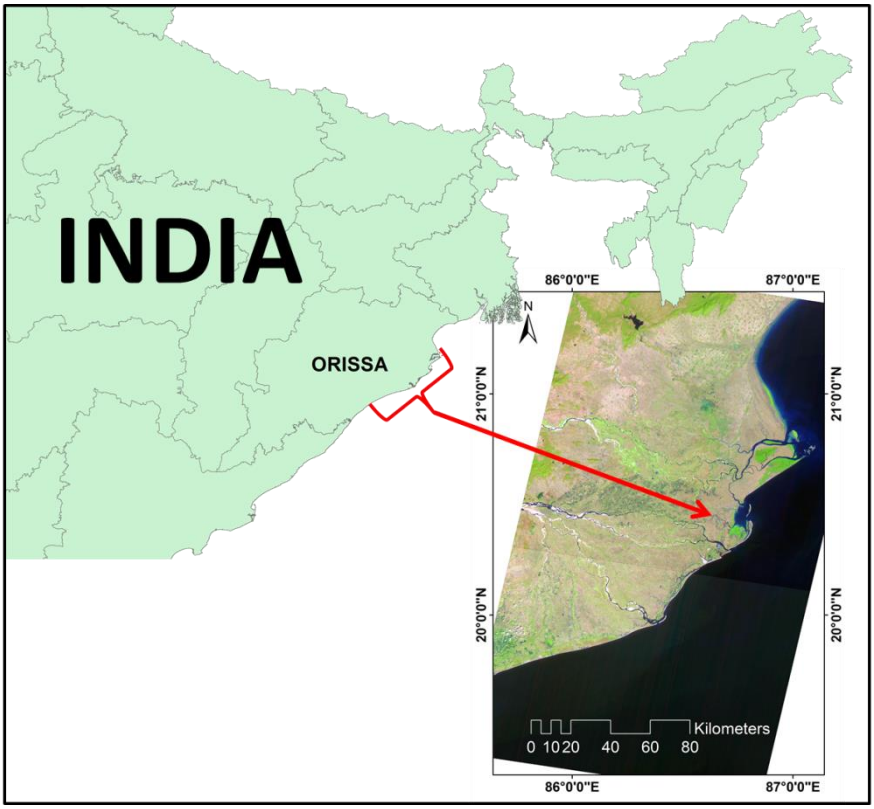

Fig. 1 The location of Mahanadi Estuary

2.2 Subdivision of the entire coastline into smaller sections

The coastline under study was divided spatially into 9 smaller sections, namely 'A', 'B', 'C', 'D', 'E', 'F', 'G', 'H' and 'I' (Fig. 2). These divisions were made in such a way so that each division starts from a specific geomorpoholical feature like mouth a river or lake to another. This has been done for the ease of analysis and reference. Section A denotes the stretch from the mouth of Chilika Lake to the mouth of Dhaudia River (covering ≈11.76 km) and has a wide range of plantations such as Mango, Akashia, Casuarina, Cashew, Palm and others. Section B (located in Balukhand) runs from the mouth of Dhaudia River to the mouth of Nua Nai River (covering ≈ 12.69 km) and is in close proximity to human settlements and tourism infrastructures. Section C marks the region between the mouth of Nua Nai River and the mouth of Kushabhadra River. This

region is of immense ecological importance since Olive Ridley Sea Turtle (*Lepidochelys olivacea*) Reserve is located within this region. These are one of the most vulnerable aquatic species facing rapid extinction due to human activities (Seminoff and Shanker, 2008; Wallace et al., 2011). This portion of the coastline is 12.93 km long and intersects the Bulakhand-Konar reserve forests. Section D (16.38 km long) covers the Chandrabhaga beach and it runs parallel to the Puri–Konark Marine Drive ending at the mouth of Kadua River. Section E lies betwen the mouth of Kadua River and the mouth of Devi River – near Jagatsinghpur Reserve Beach Forest, covering 13.51 km. Section F (17.8 km long) starts at Saharabedi and ends at the Jatadhar Lake. Section G (17.5 km long) starts at the Jatadhar Lake and ends at the Mahanadi River mouth. Section H (7.71 km long) starts from Mahanadi River mouth and ends at Hetamundia. Section I (12.86 km long) runs from Gobari River near Jambu Dwip to the mouth of Brahmani River (see Table 2).

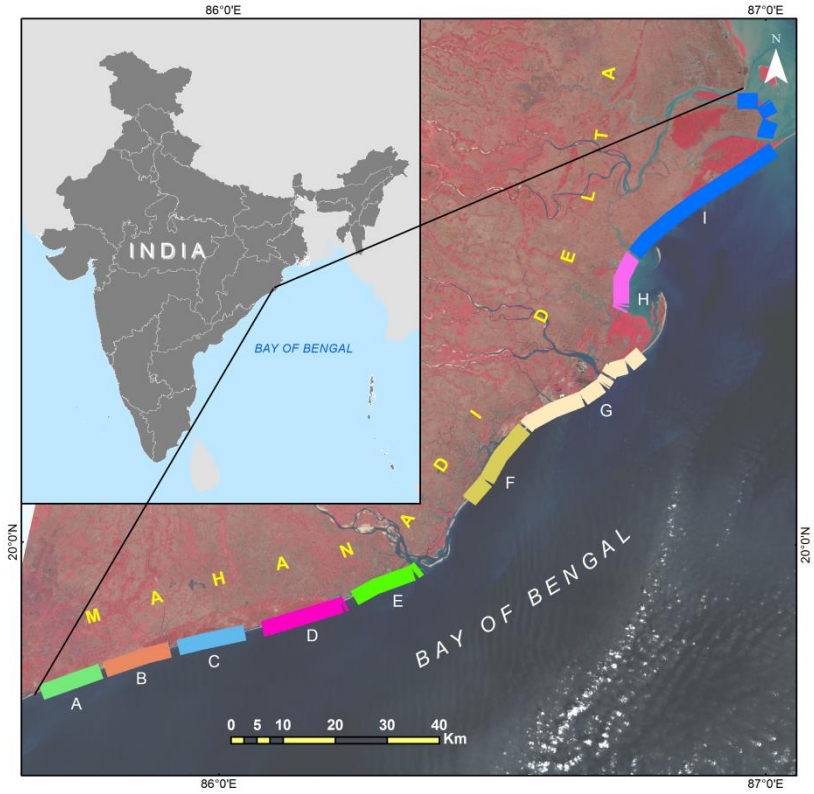

Fig. 2 The study area map of the Mahanadi Delta showing the nine subdivisions of the coastal region done for the present study

2.3 The strategy of analysis in a nutshell

LANDSAT ETM+ images were obtained from USGS GloVis and atmospheric correction was performed on it. The shorelines were extracted from the images using 'Tasselled Cap Transformation' technique and subsequently converted to vector format. A baseline was chosen on the coast and transects were cast on the shorelines falling in the study area at regular intervals. Two different types of rates were calculated from the perspective of quantifying shoreline change, namely, End-Point Rate (EPR) and Linear Regression Rate (LRR). The result was validated with the original situation of coastline in the year 2015. The EPR rates were used to calculate and predict the future position of the shorelines along each transect for the years 2035 and 2050. The population data were overlaid on the predicted coastlines of the year 2035 and 2050 to understand upcoming risk to the coastal people from coastal erosion of the Mahanadi Delta (Census, 2011).

2.4 Image acquisition and Correction

Landsat data was used in this study for the years 1990, 1995, 2000, 2005, 2010 and 2015. A summary of the satellite imageries used is appended in Table 1. The different bands of the images were stacked into a single image using the Layer Stack tool in ERDAS Imagine software. These images being low-level images contained haze and other atmospheric artefacts that usually cause difficulty in performing the shoreline analysis – especially during the extraction of shorelines. Thus, a plug-in to ERDAS Imagine namely Atmospheric & Topographic Correction (ATCOR), was used to remove the atmospheric effects.

206 The tool was fed with the acquisition dates of the image, elevation above MSL
207 and the sun elevation angle (90° – zenith angle) was calculated for the area under
208 observation. Spectral calibration was performed with the help of reference signatures for
209 different land cover types in the image. Haze removal procedure was performed on each
210 of the images in order to obtain a clearer image. Finally, atmospheric correction was
211 performed and atmospherically corrected satellite image was obtained.

212 **Table 1** The list of satellite imageries used along with the date of acquisition and the tidal
213 condition

Year	Satellite Imagery Type	Date of acquisition	Spatial Resolution	Tide (m)
1990	Landsat TM	1990-12-23	30 m	2.26
1995	Landsat TM	1995-12-21	30 m	2.30
2000	Landsat TM	2000-12-02	30 m	2.49
2006	Landsat ETM+	2005-12-24	30 m	2.21
2010	Landsat ETM+	2010-11-04	30 m	1.90
2015	Landsat OLI	2015-12-28	30 m	2.83

214

215 Semi-automatic techniques for shoreline determination are a popular and well
216 established technique (Ryu et al., 2002; Yarmano et al., 2006). In this study, the
217 'Tasselled Cap Transformation' procedure was adopted for the purpose of coastline
218 extraction from satellite images. This technique was first used by Nandi et al. (2015).
219 Applying this technique, spectral data from six bands of the respective LANDSAT
220 imageries were projected into three principal components – brightness, greenness and
221 wetness (Crist and Sisone, 1984). The wetness index was used to differentiate land and

water quite distinctly, thereby establishing the land-water interface – which is essentially the coastline. The wetness component was then masked with a binary filter and the raster binary image was finally converted to a vector image (.shp) using ArcGIS. In Fig. 3 the vector shorelines extracted from the satellite images using Tasselled Cap technique has been shown. The insets show some selected points of interest on the shorelines at a magnified scale.

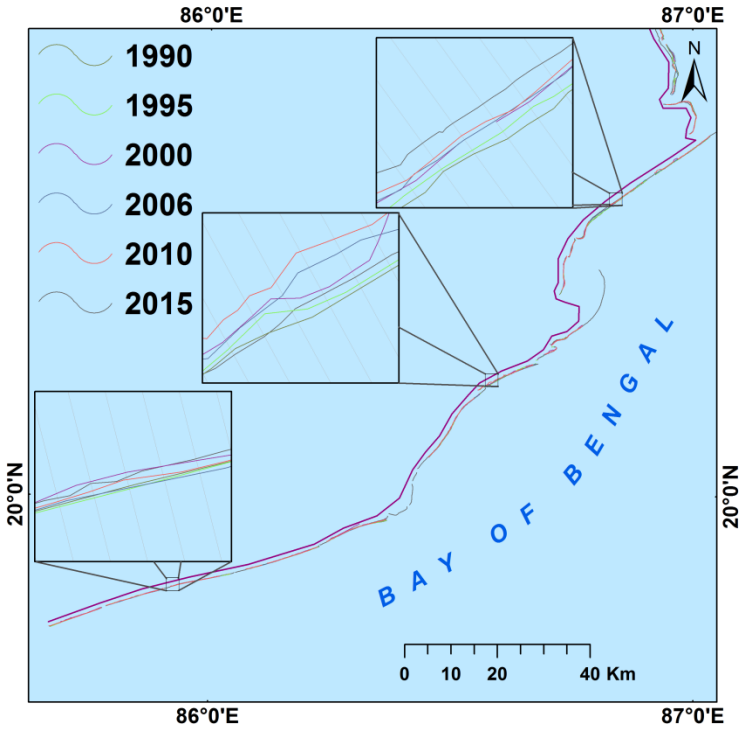

Fig. 3 Extraction of vector shorelines from the satellite images of the years 1990, 1995, 2000, 2006, 2010 and 2015 using Tasselled Cap technique

The extracted coastline was compared with the total station survey plot along some sectors of the PURI coast line towards Konarak, which have been surveyed in 2015 December. The graph showing the maximum differences between the extracted coastline and the surveyed coastline is less than 1 meter with a mean difference of 0.42 metre. As the same technique were applied on every years image so while comparing the year wise data this error would have no significance (See Graph 1 in Supplementary materials).

2.5 Choosing a baseline and transect casting using DSAS

DSAS requires a baseline and the historical shorelines with their dates as an input. The shoreline can be chosen both on and off the shore, but in this study an onshore baseline was created. A buffer of total width 1 km was generated around the shoreline corresponding to the first year – i.e., the year 1990. The buffer was so chosen that the 1990 coastline subdivides the buffer region into two equal parts. The seaward half of the buffer region – i.e., the buffer area to the right of the 1990 coastline in this case, was omitted. The polygonal feature was then converted to a polyline to obtain the baseline for the study.

The extracted shorelines were then modified so that each shoreline feature consists of a 'date' attribute. As required by DSAS, the date was provided in MM/DD/YYYY format. All these shorelines were then merged into a single feature class. The parameters for the model were provided to DSAS. They include the baseline, selected to be on-shore, transect spacing and transect length. Transect spacing and transect length were chosen to be 50 m and 2.5 km respectively. The shoreline parameters were also fed into DSAS.

2.6 Statistical Analysis of shoreline movement

In the present study two methods namely End-point Rate (EPR) and Linear Regression Rate (LRR) were implemented to delineate the shoreline change.

2.6.1 End-Point Rate (EPR)

End-point Rate (EPR) (Fenster et al., 1993) of a point on the shoreline is measured along a transect and is defined as the ratio of the net movement of the shoreline at that point along that transect in a time interval to the difference in time (usually in

years) between the two observations (i.e. the range of the time interval). Yearly EPR can thus be found by using the following equation:

$$\boldsymbol{Annual\ EPR\ (in\ m/yr)} = \frac{\boldsymbol{Distance\ of\ Shoreline\ Movement\ (in\ m)}}{\boldsymbol{Time\ elapsed\ (in\ yr)between\ the\ oldest\ and\ the\ latest\ observation}} \quad \text{.....(1)}$$

The main advantage of EPR is its ease of calculation and it shows the overall change of shoreline positions. It is thus suitable for long term prediction of future shorelines. However, since it takes into account only two shoreline positions it completely ignores the intermediate shoreline positions between the first and the last observations. As a result, cyclic trends in shoreline movement, if present, remain undetected (Crowell et al., 1997; Dolan et al., 1991).

2.6.2 Linear Regression Rate (LRR)

Linear regression rate denotes the output of a statistical computational technique which, in this case, calculates the rate of change of shoreline movement. Although the method is purely computational, it provides valuable insights to the rate of change of shorelines as it considers the shoreline data of all the years given as input. This method, calculates the rate-of-change statistics for each of the shorelines corresponding to each year at the same transect position (Temitope and Oyedotun, 2014). In simple linear regression, a model function can be written in the form,

$$h(x) = \beta_0 + \beta_1 x_i \text{.....(2)}$$

where β_0 and β_1 are unknown coefficients which are to be computed and x_i is the i^{th} observation or data – in this case i referring to the different years.

281 This corresponds to a straight line with an offset β_0 and a slope of β_1. A notion of
282 error can then be defined which in this case is chosen to be the mean squared error. A
283 cost function can defined as

284 $$J = \frac{1}{2N}\sum_{i=1}^{N}(y_i - h(x))^2 \ldots\ldots (3)$$

285 where N represents the total number of observations; y_i is the observed value of the i^{th}
286 observation. Substituting h(x) in the above equation (Eq. 3) with Eq. 2, we get:

287 $$J = \frac{1}{2N}\sum_{i=1}^{N}(y_i - \beta_1 x_i - \beta_0)^2 \ldots\ldots\ldots\ldots (4)$$

288 The objective is to find the values of β_1 and β_0 for which this cost function (J) is
289 minimized. The line plotted with these parameters β_0 and β_1 as the offset and the slope
290 respectively gives the best fit line for the data., thus calculating the rate of change in the
291 positions of the shoreline. The main disadvantage of this method is that it is prone to
292 outlier effects and might be over-influenced by shoreline points which are significantly
293 out-of-line in comparison to temporally-closer neighbouring data points.

294 **2.7 Validation and prediction accuracy**

295 In order to validate the automatic shoreline extraction a Landsat OLI data was
296 digitized manually. This digitized data was compared with the shoreline calculated
297 automatically from the tasselled cap technique to establish the correctness of the method.
298 In this study images of the years 1990, 1995, 2000, 2006 and 2010 were used to predict
299 the future coastlines of the study region (discussed in details in section 3.6). In order to
300 validate the predicted outcome we have calculated the expected shoreline for 2015
301 (separately for each transect), according to the established method. The positional
302 difference between the expected and actual positions (obtained from the tasselled cap

technique) was calculated and compared statistically with the actual position to establish the validity of the rates.

2.8 Prediction of future shoreline position

As the EPR showed better result for the calculation of the future coastline the EPR rates were used by extending the last shoreline; i.e., of the year 2015, along each transect. Thus, a point was generated for each transect according to the following equations (Stancioff et al., 2017):

$$I_x = x + r\Delta t \times \cos\left(\tan^{-1}\left(\frac{y-y_0}{x-x_0}\right)\right) \ldots\ldots(4)$$

$$I_y = y + r\Delta t \times \sin\left(\tan^{-1}\left(\frac{y-y_0}{x-x_0}\right)\right) \ldots\ldots(5)$$

where

I_x = x-coordinate of the predicted shoreline point

I_y = y-coordinate of the predicted shoreline point

x = x-coordinate of the intersection of the transect with the last shoreline (2015)

y = y-coordinate of the intersection of the transect with the last shoreline (2015)

r = Rate of change of shoreline (measured here by EPR or LRR in m/yr)

Δt = Time difference (in yr) between the year for which prediction is needed and the last year (2015)

$\tan^{-1}()$ = Inverse tangent function also denoted as arctan()

y_0 = y-coordinate of the intersection of the transect with the first shoreline (1990)

x_0 = x-coordinate between the intersection of the transect with the first shoreline (1990)

The reason behind the formulation of the equations has been explained in Fig. 4. In this figure an arbitrary case showing an EPR of -0.2m yr^{-1} signifying erosion is discussed. The blue curve denotes the current shoreline of 2015. The baseline from which transect has been drawn is shown in red. Transect has been shown in black. While predicting the shoreline position after 10 years, i.e., in the year 2025, the following points need to be considered. The net shoreline movement in these 10 years was $-0.2\ m/yr \times 10yr = -2m$. If the x- and y-coordinates were decreased by this amount to predict the future position – an error would have incurred as the erosion, or accretion for that matter, is measured along transect. Thus, the angle the transect makes with the projected coordinate system's (UTM) grid needs to be taken into account. If the x-coordinate decreased from the point A to point C, and y-coordinate from point A to point B with AC = AB = 2m then, the predicted point should come to point D, which is erroneous. This 2m should insteadbe measured along transect as the rate of erosion (or accretion) itself is defined along transect. Measuring this distance along the transect, the point was determined to be point E, which is situated at the point of intersection of the transect with the circle passing through points B and C with point A as the centre – i.e. a circle with a radius equal to the net shoreline movement.

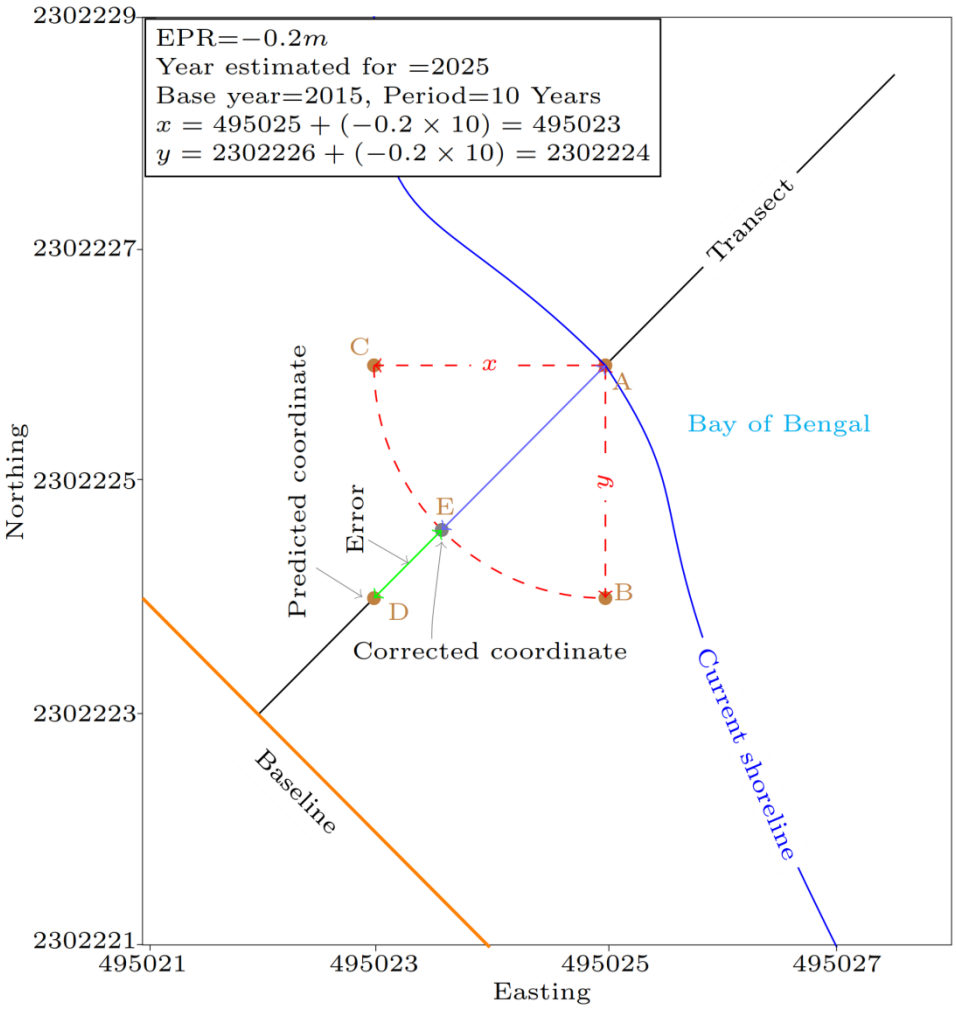

340

341 **Fig. 4** An illustration showing an arbitrary case having an EPR of -0.2m/yr signifying
342 erosion with relation to the mathematical equations adopted for the present study

343 The cosine and sine functions take the argument of the angle of a transect with
344 respect to the x-axis of the UTM grid. This quantity was derived as follows. Let the slope
345 of a transect be m. Then taking the intersection of the first shoreline (1990) and the
346 transect as the origin, the transect can be represented by the equation,

347 $$y = mx + c \quad \ldots\ldots\ldots (6)$$

348 This is the general equation of a straight line in slope-intercept form. The
349 intercept (c) is zero in this case since the intersection is being considered the origin but

has been retained to preserve generality. Here y is the y-coordinate of the intersection of the transect with the last shoreline (2015) and x is the x-coordinate of the intersection of transect with the last shoreline (2015). Similarly, for the intersection of the first shoreline and transect, the y-coordinate (y_0) can be written as the function of the x-coordinate (x_0) as follows:

$$y_0 = mx_0 + c \text{.....} (7)$$

Here m remains the same since they both represent the same straight line – i.e. transect. Now, subtracting the second equation from the first, we get,

$$y - y_0 = m(x - x_0) \text{.....} (8)$$

$$m = \frac{y-y_0}{x-x_0} \text{.....} (9)$$

The equation of transect can also be written in terms of the angle with the x-axis, θ, as follows:

$$m = \tan\theta = \frac{y-y_0}{x-x_0} \text{.....} (10)$$

Thus, θ can be calculated as,

$$\theta = \tan^{-1}\left(\frac{y-y_0}{x-x_0}\right) \text{.....} (11)$$

Thus, the angle a transect makes with the x-axis of the grid can be found in terms of the x and y coordinates. The cosines and the sines of this angle are multiplied with the net shoreline movement ($r\Delta t$) and added to the x and y coordinates of the intersection of the last shoreline and the transect respectively to yield the predicted coordinates.

These points, obtained for each of the transects were joined to form a curve representing the future predicted shoreline.

3. Results and discussion

3.1 Comparative analysis between EPR and LRR

Previous literature showed mixed opinions on the performance of EPR and LRR in shoreline change analysis. Sutinko et al. (2016) and Islam et al. (2014) found no such significant difference between EPR and LRR. Dean & Malakar (1999) preferred LRR to EPR. Cases where LRR was preferred can also be found. Even though different statistical methods exist to analyse shoreline change, the authors of this article would like to vote strongly for End-Point Rate for long-term shoreline analysis due to its accuracies in prediction, consistency, simple calculation procedure and ease of communicating and understanding. Even though, EPR takes into account only the first and the last available shoreline position data, the results are quite good as seen from its validation. The inclusion of the trigonometric factors while predicting the future point for the coastline reduces some of the inaccuracies that might have been associated with EPR-based (as well as those based on other statistics, including LRR) predictions. The authors believe the equations proposed here to be more correct – conceptually as well as the accuracy of the results obtained – and that exclusion of these trigonometric factors would lead to erroneous results. Even though these terms have not been used extensively in previous literature, this study proposes and recommends these correction terms for future studies.

It was observed that the 2015 shorelines as predicted from the EPR and LRR rates were very close to the actual shoreline of 2015 (Fig. 5). Moreover, the EPR and LRR points themselves were found to be in good agreement with each other as seen from the map. The green dots representing points predicted with EPR were found to be almost superimposed on the red dots representing points predicted with LRR (Fig. 5). The scale bar corresponds to the map scale in the insets. However, the statistical measures of the

deviation from the actual shoreline depicted in Fig. 6 enabled us to minutely differentiate between the two methods. The minimum deviation from the observed points for both EPR and LRR rates were quite low (9.7×10^{-3} m and 0.32 m respectively). However, when considering the maximum deviation for these rates, LRR exhibited a poor performance (343.9 m) but EPR delivered a relatively better result of 7.1 m deviation from the actual point. Consequently, the mean deviation was also high for LRR (24.5 m) in comparison to that of EPR (3.5 m) as there were a number of outliers having a large absolute deviation. It was also noticed that these outliers for LRR occurred mostly on the sharp bends and fragmented shoreline sections. These usually corresponded to river mouths and backwaters in the region. It was inferred that EPR gave consistently better results when compared to LRR. Stancioff et al. (2018) while characterizing the shoreline change of St. Kitts Island in the Caribbean studied only under the business-as-usual scenario as adopted in this paper and they also observed EPR to be a suitable tool for addressing the changes in shoreline dynamics. Even though at some points the positions derived from LRR closely matched the original shoreline position, its inaccuracy in deriving rates for a rough and unsmooth coastline which is a common feature, prompted us to use EPR instead of LRR while predicting the future shoreline. However, there are studies conducted in the very east coast of India (state of Tamil Nadu), where both LRR and EPR method exhibited identical results (Sheikh and Chandrasekar, 2011). In another recent study conducted in the Tamil Nadu state, LRR and EPR exhibited similar results (Natesan et al., 2015). Thus it can be deduced that the applicability of the methods adopted might significantly vary spatially.

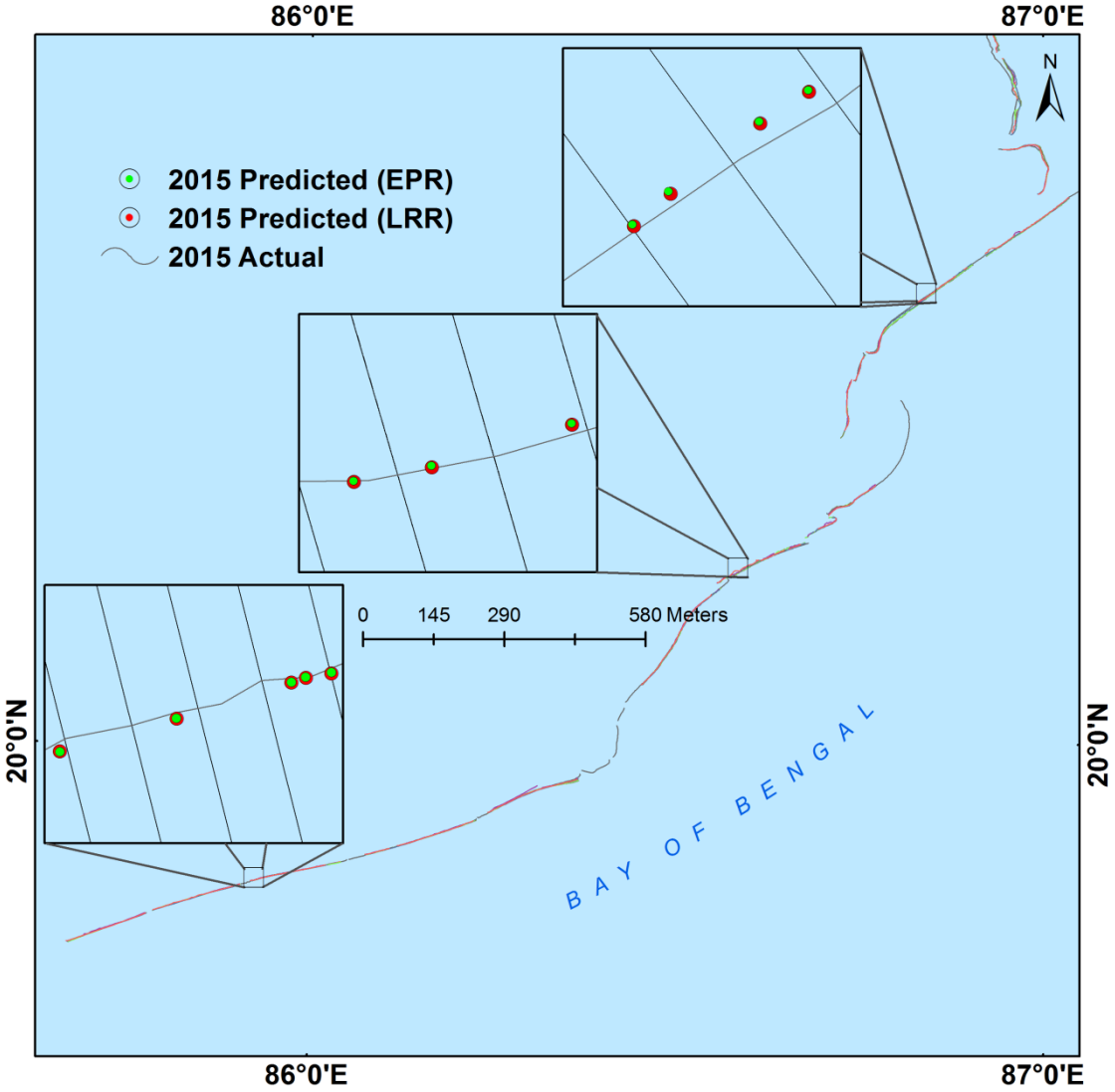

419

420 **Fig. 5** Predicted coastal points by the LRR and EPR methods in the image for the year

421 2015

422

423

424

425

426

Table 2 The mean ± standard deviation and median erosion rate observed from both EPR and LRR method in the all the subdivisions of the study area

Section	Transect # (from)	Start Point	Transect # (to)	End Point	Mean EPR (m/yr)	Median EPR (m/yr)	SD EPR (m/yr)	Mean LRR (m/yr)	Median LRR (m/yr)	SD LRR (m/yr)
A	1	Mouth of Chilka	60	Mouth of Dhaudia	-9.20	-1.26	18.43	5.01	0.48	5.92
B	66	Mouth of Dhaudia	130	Mouth of Nua Nai	15.22	-0.58	59.15	6.94	-0.69	40.00
C	140	Mouth of Nua Nai	204	Mouth of Kushabhadra	-1.98	-1.48	2.16	-0.69	-0.89	2.25
D	223	Chandrabagha Beach	303	Mouth of Kadua	-2.15	-1.57	5.01	-1.39	-1.32	2.88
E	314	Mouth of Kadua	380	Mouth of Devi	-2.82	-1.99	3.91	-0.56	-0.96	2.86
F	462	Saharabedi	549	Jatadhar lake	-16.33	-4.68	22.72	-9.88	-3.345	18.64
G	553	Jatadhar Lake	687	Mouth of Mahanadi	2.83	1.26	14.56	3.66	1.03	14.76
H	747	Mouth of Mahanadi	802	Hetamundia	-10.91	-8.825	12.14	-9.93	-7.12	12.12
I	806	Mouth of Gobari	1039	Mouth of Brahmani	-4.15	-5.46	11.91	-4.04	-5.13	9.72

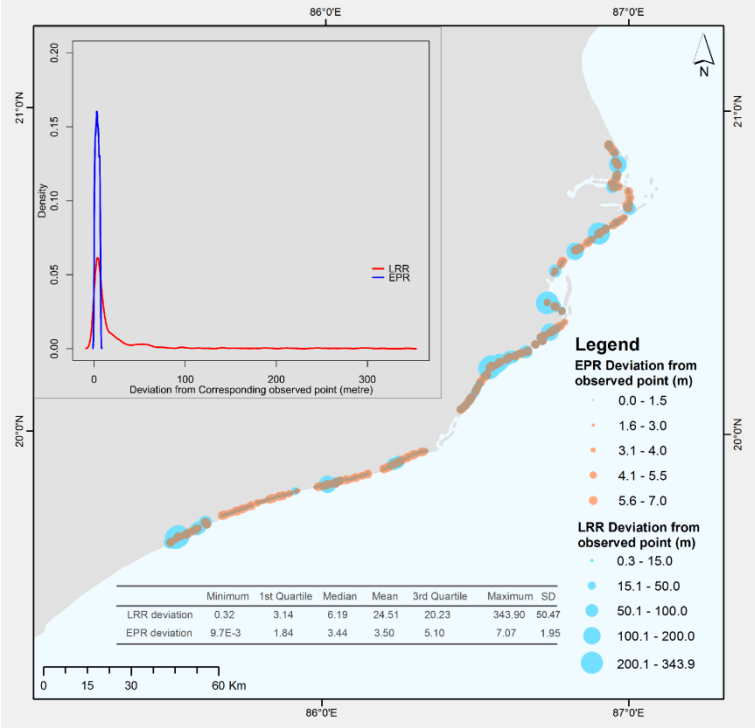

Fig. 6 Differences between the LRR and EPR methods of points extraction in the shoreline

3.2 Section wise shoreline change scenario between 1990 and 2015

The coastlines extracted from the automatic tasselled cap images were compared to the actual coastlines digitized from the Landsat satellite image for the year 2015 (Fig. 7). The intersections of transects with these two coastlines were extracted as points and compared against each other. The median values showed similar category of shoreline dynamics (i.e. erosion or accretion) for all the sections except section 'B' (Table 2). Although the mean values for both EPR and LRR were positive (implying accretion), the median values of both the rates were negative (implying erosion). This was so because, as revealed later in this paper, a small portion of the coastline underwent rapid accretion while the larger part underwent steady erosion. The detailed section-wise erosion/accretion rates of the coastlines along transect are discussed in Supplementary files (and also see Graph 2 in Supplementary files).

458 The study revealed that the southernmost coastal region of the Manhanadi delta
459 (section A) i.e. in mouth of the Chilika the rate of mean erosion is third highest and is
460 around 10 metre per year up to the mouth of river Dhaudia, where most of the coastal
461 regions are under the threat of the erosion. Here very thin coast line exists between Chilika
462 and the Bay of Bengal. The situation changes in the next section (Section B) up to the mouth
463 of the Nua Nai river where accretion plays a major role. This is the coastal region of Puri
464 city, the main tourist spot of Odisha. The reason behind this accretion may be due to the
465 recent beach nourishment activity of the authority and coastal engineering structure.
466 Similar accreation of beach due to construction of breakwaters was observed in the
467 Udayavara River mouth in the Udupi coast in the south wester coast of India (Deepika et al.,
468 2013). In the next sections C, D and E up to the river mouth of the Devi moderate erosion up
469 to 2 meter per year was noticed. The situation changes in the next section F (from
470 Saharabedi to the Jatadhar lake) the rate of erosion was found highest around 16 metre per
471 year. The concave shape of this coast line and sediment scarcity due to the coastal structure
472 near Paradwip is mainly causing erosion in this part of the coast. This situation changes in
473 the next part due to the presence of the coastal structure of the Paradwip area. This coastal
474 part is acceding on an average 3 meter per year up to the river mouth of Mahanadi. The
475 following two sections are facing erosion rate decreasing from south to north.

476 **3.3 Physical impact of shoreline change observed during the present study period**

477 It is seen from this study that the area under observation has undergone erosion on
478 an average with the maximum mean erosion rates being -16.331 m/yr. Section ‘F’ shows
479 maximum average rate of erosion whereas Section ‘C’ shows the minimum rate of
480 erosion on the average. As for the rates of accretion, minimum rate of accretion has been
481 found in Section ‘G’ and maximum accretion has occurred in Section ‘B’. Accretion has
482 occurred maximum in ‘B’ and minimum in Section ‘G’, on an average. Similar type of
483 erosion as well as accretion has also been observed in Shanghai, China based on Landsat

484 data analysis during a span of last 55 years from now (Qiao et al., 2018). Reduction in
485 sediment loading from the adjacent Yangtze River and land reclamation were mainly held
486 accountable in this study. The upstream of Mahandi has also witnessed various small
487 check dam constructions in the recent past and hence the accretion observed could as a
488 consequence to that, however, delineating the exact cause was outside the ambit of the
489 present research. However, it is worth mentioning that a sharp decrease in the sediment
490 discharge of Mahanadi has been observed recently (Bastia and Equeenuddin, 2016),
491 hence the results obtained can be justified to a large extent. It is observed that in
492 populated sections of the coastline, corresponding to major cities and tourist destinations,
493 erosion has been relatively mild in comparison to its neighbouring sections. For example,
494 in the section corresponding to Puri – a major tourist destination – the median rate of
495 erosion has been not too high (EPR = -0.58 m/yr) with mean EPR showing accretion.
496 Whereas, in neighbouring regions of Puri (especially the northern part), significant
497 erosion was observed, which was also previously reported by Mukhopadhyay et al.
498 (2012). Similarly, Paradwip (Section 'G') shows accretion at a median rate of 1.26 m/yr
499 (EPR). Only two major towns – Konark and Gopalpur – show erosion at a significant
500 rate. Konark (Section 'D') shows erosion at a median rate of -1.57 m/yr (EPR) while
501 Gopalpur (Section 'I') shows a rate of -5.46 m/yr (EPR). Zhang et al. (2004) while
502 analysing a global erosion model observed that in the last century global erosion rate as
503 high as 20 m/yr in some coastlines. In a similar delta like that of Nile Delta, Smith and
504 Abdel-Kader (1988) observed an erosion rate of 35-50 m/yr in the end of 20th century.
505 Nassar et al. (2018) in a similar study carried out in the North Sinai coast of Egypt
506 observed erosion rate varying from 2.9-8.65m/yr. Compared to these studies we found
507 that in some of the transects of Mahanadi Delta erosion was much more than that
508 observed in the Nile, whereas the mean rate was found to be -16.33 m/yr. Hence, we can

successfully accept our proposed hypothesis that Mahanadi delta is undergoing erosion at par with the global rate and in some transects even more than the global average erosion rate.

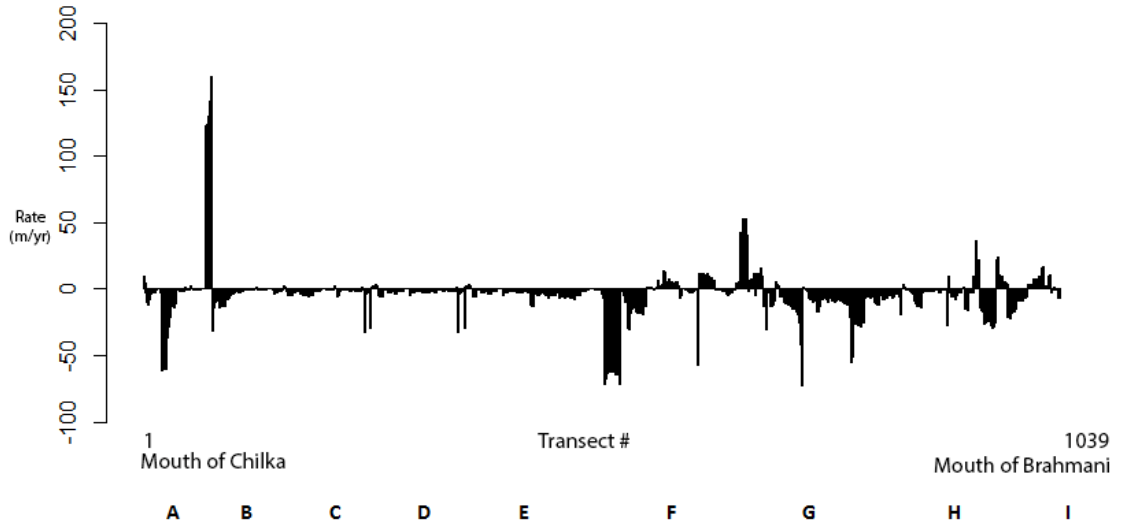

Fig. 7 The erosion and or accretion rate observed for all the transects during the study period by EPR method

3.4 Social impact of shoreline movement

Coastal ecosystem is a vulnerable one because of its dynamic nature attributed to frequent erosion and accretion. In the state of Orissa, a number of villages, towns and cities are situated along the coastline in the Mahanadi Delta. With an average population density ranging from 250-1000 persons per sq. km., it is one of the most populous coastlines in India (Census, 2011). In the lesser educated societies in this delta, especially in the tribal communities, the literacy rate has been quite low and as a result, they – mostly the women – resort to unskilled labour to meet their daily needs. Catering to tourists in the area being one of the most prominent aspects of their livelihood, which

524 includes selling products and services, rapid erosion and degradation of the shoreline
525 indirectly affect their life as it is linked with the volume of tourist inflow. The spatial
526 distribution of erosion along with the household and population density is depicted in Fig.
527 8. It is seen from the administrative boundaries that few areas are having a significant risk
528 towards erosion. These coastline sections have been marked in red signifying very high
529 risk of erosion. Areas with maximum households corresponds to Puri (41150) and
530 Paradwip (17485) municipalities followed by Konark and Kapileshwar. Population
531 density is found to be very high in these regions. There are six areas with a population
532 density above 20000 persons per square kilometres. They are Gopaljew, Kasiharipur,

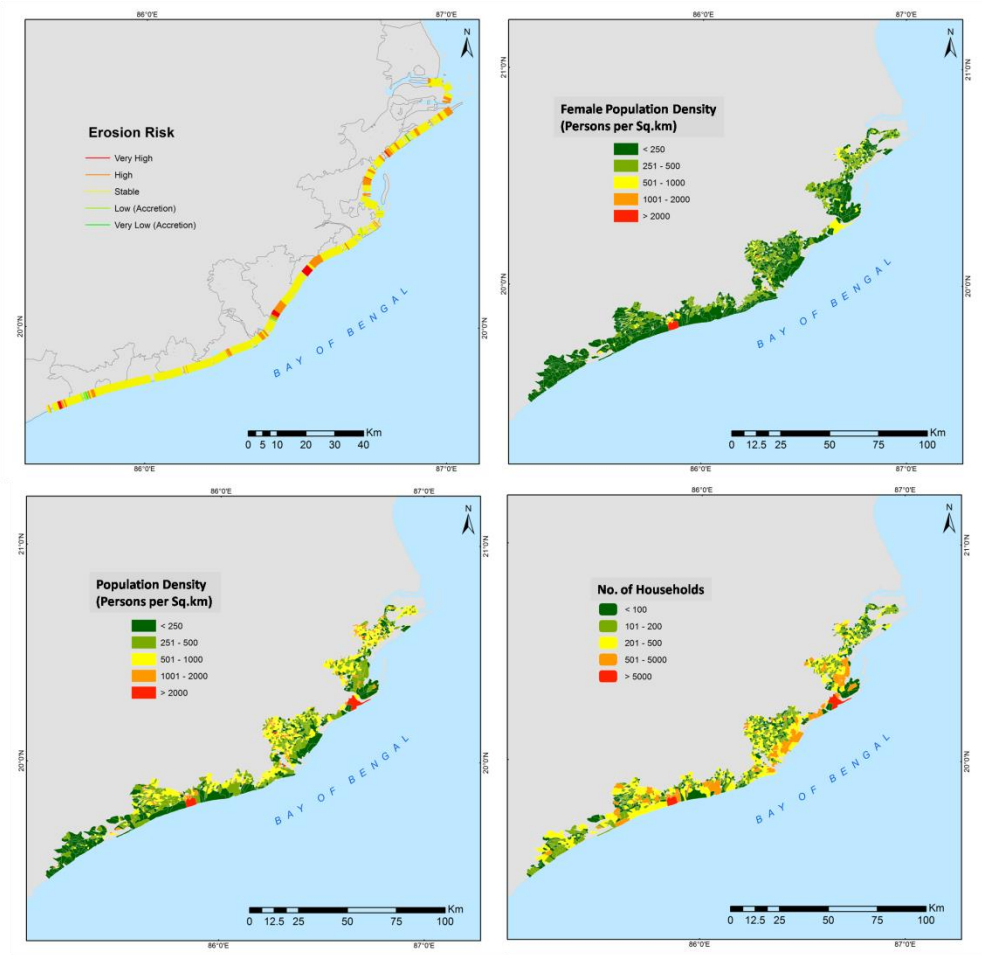

533

Fig. 8 The maps showing the variability of i) risk due to erosion, ii) population density, iii) female population density and iv) number of households in the selected study area (Data Source: Census, 2011)

Karimpur, Kanak Nagar, Atharanala and Gupti, in increasing order of population density. Among 87 Mouzas situated in the coastlines of Mahanadi 26 are under the threats of the high to very high erosion risk. More than 8000 households with population density varying from 7 to 1690 per square km with an average of 241 persons per sq km are under direct threat to the eminent consequence of the coastal erosion. The corresponding female population densities have also been the highest in these regions. Unfortunately, Fig. 8 depicts that many of these areas are substantially affected due to erosion. In these regions, males tend to migrate to other states or regions in search of jobs whenever they face acute unemployment in their locality. Given the scenario in the region where most women have more responsibilities in their household than males, it is difficult for women, especially those who head an entire household, to migrate somewhere else. Hence the ill-effects of erosion which includes lessening of tourist inflow and damage of residential properties hurt the female section of the population more directly. The mean female population densities of the most effected 26 Mouzas are 120 persons per sq km who are going to be the most vulnerable portions of the population due to this predominant erosion threat (see supporting information Table S1). Similar observations were also reported by Cutter et al. (2003) and Terry (2009).

3.5 Predicted impact of the shoreline change for the years 2035 and 2050

Fig. 9 exhibits that almost all of the regions in close proximity to the sea face the risk of erosion by the year 2050. Puri, being a vital point of attraction in the tourism industry, it is very likely that the industry will be affected due to shoreline dynamics in

the future. Paradwip, being a known as one of the busiest port area also seems to face the same fate in the future. It is evident from both Fig. 10 and Table S1 (See Supporting Information) that a number of mouzas in the region show a high risk.

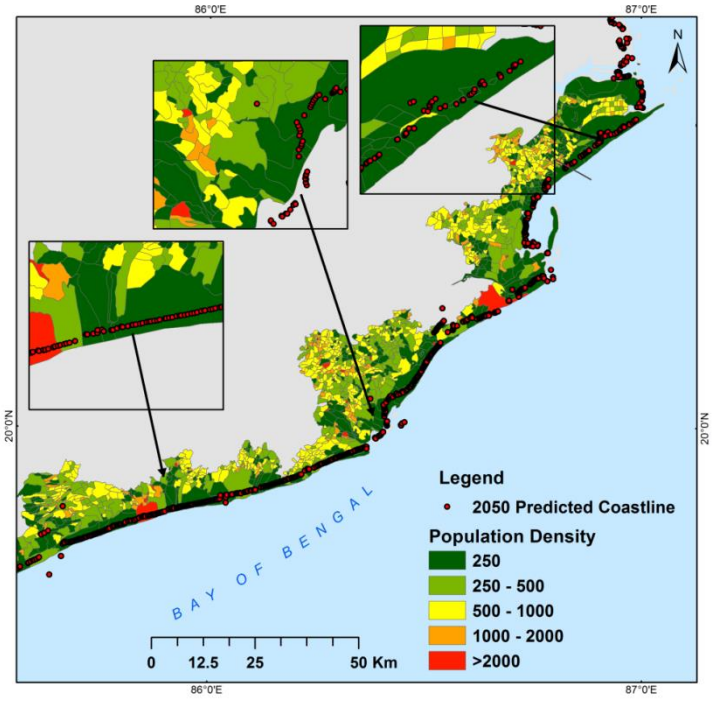

Fig. 9 The predicted coastline of the study area for the year 2050 along with the population density overlaid on the map

16 mouzas have a high risk of erosion. Long Wheeler, Gohipur, Odiasala, Firikichhitakandha, Panigadiakandha, Kanhupur, Kandara patia, Sahadabedi,

Banapatakandha, Kokakhandha, Garhkujang, Gobindapur, Jamboo, Dhinkia, Nuagan, Balitutha belong to this category. However, most of the villages have stable conditions, with a few mouzas having transects with a moderate risk of erosion. They are, Satavaya, Sipasurubili, Sudikeswar. Abadan, Badagahiramatha, Mahakaldia, Jatadhar, Harispurgarh, Jatadhartanda and Sipasurubili. It can be seen that Puri and Paradwip –

578 although having a high population density – is at a moderate level of risk. Jatadhar and
579 Harishpurgarh are seen to be at an alarming level of risk due to erosion in the region.

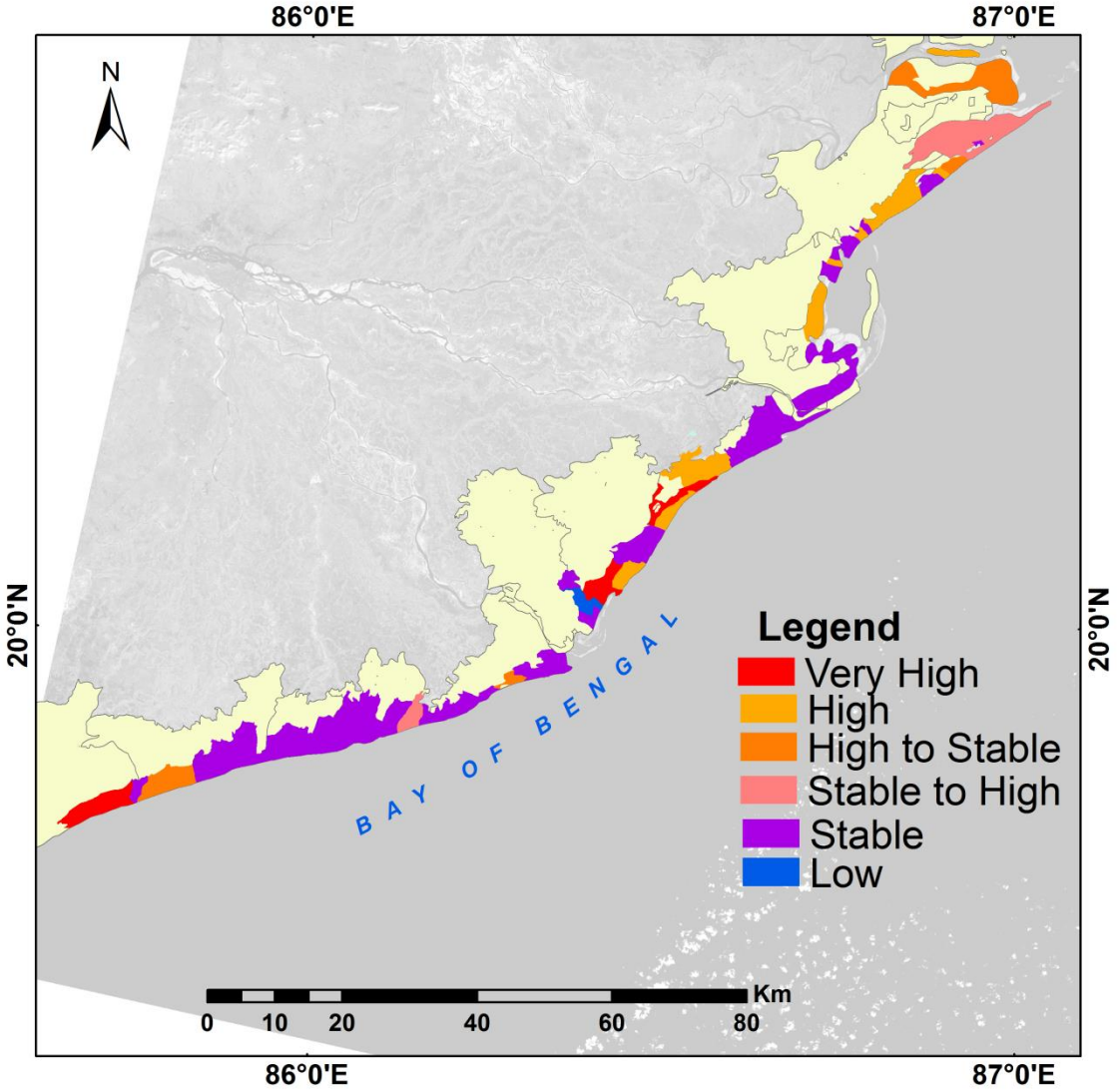

580

581 **Fig. 10** The composite risk map for the selected study area from the perspective of
582 erosion showing the spatial variability of risk throughout the coastline

583 **4. Conclusion**

584 After analysing the outcomes from the present study, it can be inferred that EPR
585 showed a better performance with respect to consistency in comparison to LRR for
586 shoreline change analysis for the coastal area of Mahandi delta. From the perspective of

erosion, it was observed that various transects in the coastline of Mahanadi delta are, at present, undergoing unprecedented erosion at an alarming rate and the predicted coastline for the year 2050 showed that it would only worsen in the future. Several regions having high tourist inflow would be hit hard due to the on-going erosion in the future, especially where the female population density and household density are on the higher side. The predicted outcomes show that about 30% of the total coastal mouzas are going to experience the threats of high to very high erosion risk. At present close to 8000 households are under very high risk from the perspective of erosion. Going by the increasing trend of population in this part of the world, it can be said that the imminent risk of erosion will be experienced by many more number of households in near future.

This study established a long-term prediction model of erosion risk of coastal part of Mahanadi delta that can help in both prevention as well as taking steps to estimate a time-period by which alternatives could be found in case of failing to stop the erosion in high-risk zones. This includes relocation of population from mouzas which are under imminent threat from coastal erosion. This study also specifically identified such *mouzas* (small administrative blocks) in which this relocation program is to be carried out (high to very high risk zones). In addition, it also proposes villages under moderate threat where prevention strategies are to be implemented with immediate effect to nullify the need for such relocation in the near future.

Acknowledgments

This work is carried out under the Deltas, vulnerability and Climate Change: Migration and Adaptation (DECCMA) project (IDRC 107642) under the Collaborative Adaptation Research Initiative in Africa and Asia (CARIAA) programme with financial support from the UK Government's Department for international Development (DFID) and the

611 International Development Research Centre (IDRC), Canada. The views expressed in this
612 work are those of the creators and do not necessarily represent those of DFID and IDRC
613 or its Boards of Governors carry out the present work. Authors are also grateful to
614 OSDMA , CDA,USGS, NASA for providing the help and data required.

615 **References**

616 Addo, K.A., Walkden, M. and Mills, J.P.T., 2008. Detection, measurement and prediction
617 of shoreline recession in Accra, Ghana. ISPRS Journal of Photogrammetry and Remote
618 Sensing, 63(5), pp.543-558.

619 Al Bakri, D., 1996. A geomorphological approach to sustainable planning and
620 management of the coastal zone of Kuwait. Geomorphology, 17(4), pp.323-337.

621 Albert, P. and Jorge, G., 1998. Coastal changes in the Ebro delta: Natural and human
622 factors. Journal of Coastal Conservation, 4(1), pp.17-26.

623 Bastia, F., & Equeenuddin, S. M. (2016). Spatio-temporal variation of water flow and
624 sediment discharge in the Mahanadi River, India. Global and Planetary Change, 144, 51-
625 66.

626 Church, J.A., White, N.J., Aarup, T., Wilson, W.S., Woodworth, P.L., Domingues, C.M.,
627 Hunter, J.R. and Lambeck, K., 2008. Understanding global sea levels: past, present and
628 future. Sustainability Science, 3(1), pp.9-22.

629 Church, J.A., White, N.J., Coleman, R., Lambeck, K. and Mitrovica, J.X., 2004.
630 Estimates of the regional distribution of sea level rise over the 1950-2000 period. Journal
631 of climate, 17(13), pp.2609-2625.

632 Crist, E.P. and Cicone, R.C., 1984. A physically-based transformation of Thematic
633 Mapper data---The TM Tasseled Cap. IEEE Transactions on Geoscience and Remote
634 sensing, (3), pp.256-263.

635 Crowell, M., Douglas, B.C. and Leatherman, S.P., 1997. On forecasting future US
636 shoreline positions: a test of algorithms. Journal of Coastal Research, pp.1245-1255.

637 Cutter, S. L., Boruff, B. J., & Shirley, W. L. (2003). Social vulnerability to environmental
638 hazards. Social science quarterly, 84(2), 242-261.

639 Dean, R.G. and Malakar, S.B., 1999. Projected flood hazard zones in Florida. Journal of
640 Coastal Research, pp.85-94.

641 Dolan, R., Fenster, M.S. and Holme, S.J., 1991. Temporal analysis of shoreline recession
642 and accretion. Journal of coastal research, pp.723-744.

643 Dolan, R., Fenster, M.S. and Holme, S.J., 1991. Temporal analysis of shoreline recession
644 and accretion. Journal of coastal research, pp.723-744.

645 Ericson, J.P., Vörösmarty, C.J., Dingman, S.L., Ward, L.G. and Meybeck, M., 2006.
646 Effective sea-level rise and deltas: causes of change and human dimension implications.
647 Global and Planetary Change, 50(1-2), pp.63-82.

648 Feagin, R.A., Sherman, D.J. and Grant, W.E., 2005. Coastal erosion, global sea-level rise,
649 and the loss of sand dune plant habitats. Frontiers in Ecology and the Environment, 3(7),
650 pp.359-364.

651 Fenster, M.S., Dolan, R. and Elder, J.F., 1993. A new method for predicting shoreline
652 positions from historical data. Journal of Coastal Research, pp.147-171.

653 Fletcher, C., Rooney, J., Barbee, M., Lim, S.C. and Richmond, B., 2003. Mapping
654 shoreline change using digital orthophotogrammetry on Maui, Hawaii. Journal of Coastal
655 Research, pp.106-124.

656 Ford, M., 2013. Shoreline changes interpreted from multi-temporal aerial photographs
657 and high resolution satellite images: Wotje Atoll, Marshall Islands. Remote Sensing of
658 Environment, 135, pp.130-140.

659 Hazra, S., Ghosh, T., DasGupta, R. and Sen, G., 2002. Sea level and associated changes
660 in the Sundarbans. Science and Culture, 68(9/12), pp.309-321.

661 Hengl, T., Heuvelink, G.B. and Rossiter, D.G., 2007. About regression-kriging: from
662 equations to case studies. Computers & Geosciences, 33(10), pp.1301-1315.

663 Huq S, Ali SI, Rahman AA (1995) SLR and Bangladesh: a preliminary analysis. J Coast
664 Res 44–53 doi:10.2307/25735700

665 India Register General and Census Commissioner. (2011). Population enumeration data
666 (final population). Retrieved from
667 http://www.censusindia.gov.in/2011census/population_enumeration.html

668 Islam, M.A., Hossain, M.S., Hasan, T. and Murshed, S., 2014. Department of Geology,
669 University of Dhaka, Dhaka-1000, Bangladesh. Bangladesh J. Sci. Res, 27(1), pp.99-108.

670 Jana, A. and Bhattacharya, A.K., 2013. Assessment of coastal erosion vulnerability
671 around Midnapur-Balasore Coast, Eastern India using integrated remote sensing and GIS
672 techniques. Journal of the Indian Society of Remote Sensing, 41(3), pp.675-686.

673 Kumar, A. and Jayappa, K.S., 2009. Long and short-term shoreline changes along
674 Mangalore coast, India.

675 Kumar, A., Narayana, A.C. and Jayappa, K.S., 2010. Shoreline changes and morphology
676 of spits along southern Karnataka, west coast of India: a remote sensing and statistics-
677 based approach. Geomorphology, 120(3), pp.133-152.

678 Kumar, K.V. and Bhattacharya, A.S.I.S., 2004. Remote Sensing of Delta Progradation in
679 Mahanadi Delta, Orissa. *Journal-Geological Society of India*, *64*(2), pp.227-230.

680 Kumar, T.S., Mahendra, R.S., Nayak, S., Radhakrishnan, K. and Sahu, K.C., 2010.
681 Coastal vulnerability assessment for Orissa State, east coast of India. Journal of Coastal
682 Research, pp.523-534.

683 Lovelock CE et al (2015) The vulnerability of Indo- Pacific mangrove forests to SLR.
684 Nature 526:559. doi:10.1038/nature15538

685 Mahalik, N. K., Da, C. and Maejima, W., 1996. Geomorphology and Evolution of the
686 Mahanadi Delta, India. Journal of Geosciences-Osaka City University, 39, pp.111-122

687 Mahalik, N.K., 2000. Mahanadi Delta: geology, resources & biodiversity. AIT Alumni
688 Association, India Chapter.

689 Mukhopadhyay, A., Mukherjee, S., Mukherjee, S., Ghosh, S., Hazra, S., & Mitra, D.
690 (2012). Automatic shoreline detection and future prediction: A case study on Puri Coast,
691 Bay of Bengal, India. European Journal of Remote Sensing, 45(1), 201-213.

692 Nandi, S., Ghosh, M., Kundu, A., Dutta, D. and Baksi, M., 2016. Shoreline shifting and
693 its prediction using remote sensing and GIS techniques: a case study of Sagar Island,
694 West Bengal (India). Journal of Coastal Conservation, 20(1), pp.61-80.

695 Narayana, A.C. and Priju, C.P., 2006. Landform and shoreline changes inferred from
696 satellite images along the central Kerala coast. JOURNAL-GEOLOGICAL SOCIETY
697 OF INDIA, 68(1), p.35.

698 Nassar, K., Mahmod, W. E., Fath, H., Masria, A., Nadaoka, K., & Negm, A. (2018).
699 Shoreline change detection using DSAS technique: Case of North Sinai coast, Egypt.
700 Marine Georesources & Geotechnology, 1-15. https://doi.org/10.1080/1064119X.2018.
701 1448912

702 Natesan, U., Parthasarathy, A., Vishnunath, R., Kumar, G. E. J., & Ferrer, V. A. (2015).
703 Monitoring longterm shoreline changes along Tamil Nadu, India using geospatial
704 techniques. Aquatic Procedia, 4, 325-332.

705 Oyedotun, T.D., 2014. Shoreline geometry: DSAS as a tool for historical trend analysis.
706 British Society for Geomorphology, Geomorphological Techniques. ISSN, pp.2047-
707 0371.

708 Pfeffer, W.T., Harper, J.T. and O'Neel, S., 2008. Kinematic constraints on glacier
709 contributions to 21st-century sea-level rise. Science, 321(5894), pp.1340-1343.

710 Qiao, G., Mi, H., Wang, W., Tong, X., Li, Z., Li, T., Liu, S., Hong, Y. (2018). 55-year
711 (1960–2015) spatiotemporal shoreline change analysis using historical DISP and Landsat
712 time series data in Shanghai. International Journal of Applied Earth Observation and
713 Geoinformation, 68, 238-251.

714 Rahmstorf, S., 2007. A semi-empirical approach to projecting future sea-level rise.
715 Science, 315(5810), pp.368-370.

716 Ryu, J.H., Won, J.S. and Min, K.D., 2002. Waterline extraction from Landsat TM data in
717 a tidal flat: a case study in Gomso Bay, Korea. Remote Sensing of Environment, 83(3),
718 pp.442-456.

719 Seminoff, J.A. and Shanker, K., 2008. Marine turtles and IUCN Red Listing: a review of
720 the process, the pitfalls, and novel assessment approaches. Journal of Experimental
721 Marine Biology and Ecology, 356(1-2), pp.52-68.

722 Sheik, M. and Chandrasekar (2011). A shoreline change analysis along the coast between
723 Kanyakumari and Tuticorin, India, using digital shoreline analysis system. Geo-spatial
724 Information Science, 14(4), 282-293.

725 Sherman, D.J. and Bauer, B.O., 1993. Coastal geomorphology through the looking glass.
726 Geomorphology, 7(1-3), pp.225-249.

727 Smith, S. E., & Abdel-Kader, A. (1988). Coastal erosion along the Egyptian delta.
728 Journal of Coastal Research, 4(2):245-255.

729 Somanna, K., Reddy, T.S. and Rao, M.S., Geomorphology and Evolution of the Modern
730 Mahanadi Delta Using Remote Sensing Data.

731 Stancioff, C. E., Vermeer, J., Mukhopadhyay, A., de Ruiter, S., Brown, G., & Hofman, C.
732 L. (2018). Predicting coastal erosion in St. Kitts: Collaborating for nature and culture.
733 Ocean & Coastal Management. 156, 156-169

734 Sutikno, S., 2016. Integrated Remote Sensing and GIS for Calculating Shoreline Change
735 in Rokan Estuary. KnE Engineering, 1(1).

736 Syvitski, J.P., Kettner, A.J., Overeem, I., Hutton, E.W., Hannon, M.T., Brakenridge,
737 G.R., Day, J., Vörösmarty, C., Saito, Y., Giosan, L. and Nicholls, R.J., 2009. Sinking
738 deltas due to human activities. Nature Geoscience, 2(10), p.681.

739 Terry, G. (2009). Climate change and gender justice. Oxham GB, pp. 212.

740 Thieler, E.R. and Danforth, W.W., 1994. Historical shoreline mapping (I): improving
741 techniques and reducing positioning errors. Journal of Coastal Research, pp.549-563.

742 Wallace, B.P., DiMatteo, A.D., Bolten, A.B., Chaloupka, M.Y., Hutchinson, B.J., Abreu-
743 Grobois, F.A., Mortimer, J.A., Seminoff, J.A., Amorocho, D., Bjorndal, K.A. and
744 Bourjea, J., 2011. Global conservation priorities for marine turtles. PloS one, 6(9),
745 p.e24510.

746 Zhang, K., Douglas, B. C., & Leatherman, S. P. (2004). Global warming and coastal
747 erosion. Climatic Change, 64(1), 41-58.

748 Zuzek, P.J., Nairn, R.B. and Thieme, S.J., 2003. Spatial and temporal considerations for
749 calculating shoreline change rates in the Great Lakes Basin. Journal of Coastal Research,
750 pp.125-146.